EXPERIMENTAL DEMONSTRATION OF DIFFERING IMPACTS OF PULSED AND CONTINUOUS OPERATION OF A DEUTERIUM-TRITIUM NEUTRON SOURCE ON INDUCED RADIOACTIVITY IN THE CONTEXT OF ITER

Anil Kumar[a], Yujiro Ikeda[b], Mahmoud Z. Youssef[a], Mohamed A. Abdou[a], Yoshitomo Uno[b], and Hiroshi Maekawa[b]

[a]School of Engineering and Applied Science
University of California at Los Angeles (UCLA)
Los Angeles, CA 90095
(310)825-8627

[b]Department of Reactor Engineering
Japan Atomic Energy Research Institute
Tokai-mura, Ibaraki-ken 319-11, Japan
(292)82-6074

ABSTRACT

The work reported herein was conducted in response to an ITER Task to demonstrate experimentally that pulsed and continuous operations of a D-T neutron source lead, in general, to differing impacts on inventory of induced radioactivity, on one hand, and to verify calculational methods, on the other. In a series of experiments conducted for the purpose, half lives of observed radioisotopes varied from 1 minute (^{25}Na) to 271 days (^{57}Co). Relatively short pulse lengths, 1 minute to 3 minute duration, were chosen. A pneumatic transport system was employed to transport foils of niobium, iron, aluminum, vanadium, nickel, and magnesium for irradiation close to the D-T neutron source. Three duty factors and two kinds of power levels were used for various neutron pulse trains.

The experimental data was processed to obtain ratio of inventories in pulsed to continuous operation scenarios for each of the observed radioisotope. We observe a large reduction in radioactive inventories for values of $t_{1/2}/p$ (half life/pulse duration) lying in the range of 1 to 10. Interestingly, random power pulse trains show even larger reduction in radioactive inventory: the ratio of inventories drops to ~0.14 for $t_{1/2}/p = 3.15$ (^{27}Mg) for a duty factor of 20% and a train of 10 pulses, whereas it would have hit a minimum of 0.33 for $t_{1/2}/p = 3.53$ for constant power level.

I. INTRODUCTION

The selection of materials and design options for fusion device components, including ITER, depends critically on the level of radioactivity and decay-heat induced in the components due to D-T neutron irradiation[1]. For credible design calculations, it is important to take into account probable operational scenarios of the device under consideration, as the amount of radioactivity produced depends on duty factor, length of total operation time, and power levels of component pulses, among others[2-5]. Of late, calculational methods to treat pulsed operational scenarios more accurately, on one hand, and apply them cost effectively to the existing radioactivity codes, on the other, have been reported[3,4]. From experimental standpoint, recent efforts to measure D-T neutron induced radioactivities had been built around quasi-constant source neutron output, even as impact of all variations in source neutron intensity on induced radioactivity had been explicitly and accurately accounted for[6]. The focus of the present task was placed on developing the technique for application to pulsed operation and then demonstrating its application[7].

The basic considerations requiring development of this technique are clarified through presentation of a calculational method in the following section. Note that similar results have earlier been reported in many publications- references 8 through 11 being more recent. The calculational methods/considerations, to account for time dependence of source neutron intensity on induced radioactivity, have long been used routinely by countless experimenters working on induced radioactivity- references 12 through 14 providing some of the examples of recent origin.

II. CALCULATIONAL METHOD

The build up of number of radioisotopes, say, $n(t)$, induced by neutrons through its interaction

with a target nucleus, in single-step reaction mode, is governed by:

$$n(t) = n_t \langle \sigma\phi \rangle e^{-\lambda t} \int_0^t s(t') e^{\lambda t'} dt' \quad (1)$$

where $s(t')$ is source neutron intensity at time t'. n_t is number of target nuclei swept by the neutrons. $\langle \sigma\phi \rangle$ represents radioisotope production rate per neutron per target nucleus. λ is decay constant of the product. Imagine that there are N distinct time intervals where source neutron intensity, say, s_i (i=1 to N) is defined, and i'th interval has width of q_i. In this case, one can simplify Eq. (1) to get:

$$n(t) = \frac{1}{\lambda} n_t \langle \sigma\phi \rangle e^{-\lambda t} \sum_{i=1}^{N} s_i e^{\lambda \sum_{j=1}^{i} q_j} \left(1 - e^{-\lambda q_i}\right) \quad \ldots\ldots (2)$$

Let us now deal with a case of N pulses where successive pulses are separated from one another by a time interval controlled by a duty factor, say, d. Let us further assume that i'th pulse has a width of p_i. In such a case n(t) is described by:

$$n(t) = \frac{1}{\lambda} n_t \langle \sigma\phi \rangle e^{-\lambda t} \sum_{i=1}^{N} s_i e^{\lambda \sum_{j=1}^{i-1} p_j/d} \left(e^{\lambda p_i} - 1\right) \quad \ldots\ldots (3)$$

For a special case of N pulses of identical duration, say, p, and intensity (power), say, s, Eq.(3) gets simplified to:

$$n(t) = \frac{1}{\lambda} n_t \langle \sigma\phi \rangle e^{-\lambda t} s \left(e^{\lambda p} - 1\right) \frac{\left(e^{\lambda N p/d} - 1\right)}{\left(e^{\lambda p/d} - 1\right)} \quad \ldots\ldots (4)$$

For continuous operation, we obtain:

$$n(t) = \frac{1}{\lambda} n_t \langle \sigma\phi \rangle e^{-\lambda t} s \left(e^{\lambda t_r} - 1\right) \quad \ldots (5)$$

where t_r represents total irradiation time. Note that a continuous operation means operation at a duty factor of 100%. While comparing pulsed operation to continuous operation, it is crucial to clearly understand and define the latter because one could either raise or lower the generated radioactivity. In this context, let us identify three central parameters: (i)power of operation (or source neutron intensity), (ii) total fluence accumulated, and (iii) total length of time the target is exposed to the neutron source, say, total real time. We will now consider two cases for continuous operation scenarios where two of these three parameters are conserved, while the third is left to be determined by the other two.

A. First Scenario: Power and Fluence Conserved

In the first scenario, we conserve both the power and the fluence of the pulsed case, whereas total real time is deduced from these two. The product number, for the continuous operation case, is expressed as:

$$n(t) = \frac{1}{\lambda} n_t \langle \sigma\phi \rangle e^{-\lambda t} \frac{\sum_{i}^{N} s_i p_i}{\sum_{i=1}^{N} p_i} \left(e^{\lambda \sum_{i=1}^{N} p_i} - 1\right) \quad \ldots\ldots (6)$$

B. Second Scenario: Fluence and Total Real Time Conserved

In the second scenario, we conserve both the fluence and the total real time of the pulsed case, whereas the power for the continuous operation is deduced from these two. The product number, for the continuous operation case, is then expressed as:

$$n(t) = \frac{1}{\lambda} n_t \langle \sigma\phi \rangle e^{-\lambda t} \times \frac{\sum_{i}^{N} s_i p_i}{\sum_{i=1}^{N-1} p_i/d + p_N} \left(e^{\lambda \left(\sum_{i=1}^{N-1} p_i/d + p_N\right)} - 1\right) \quad \ldots\ldots (7)$$

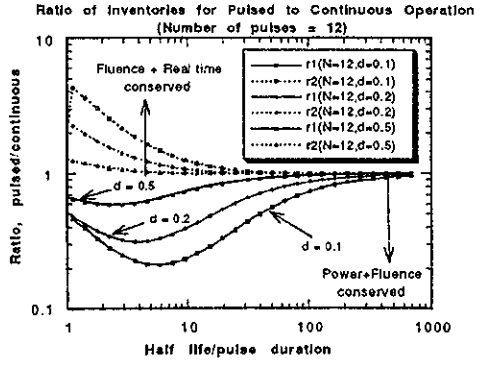

Fig. 1 Ratio of inventories for pulsed to continuous operation for a pulse train containing 12 pulses of constant power, as a function of $t_{1/2}/p$ (half life/pulse duration) and d (duty factor) for two alternative scenarios

C. Comparison of Pulsed to Continuous Operation

We have compared the decay radioactivity in a pulsed mode of operation against the two modes of continuous-operation scenarios discussed above. We assume identical pulses. The duty factor has been varied from 10% (d=0.1) to 50% (d=0.5) and the number of total pulses (N) was varied from 2 to 12. Figure 1 shows the ratios of inventories of radioactive products as a function of their half life ($t_{1/2}$), expressed in units of pulse duration, i.e., as $t_{1/2}/p$, where p is pulse duration. Note that r1 and r2 in Fig. 1 stand respectively for the first and second scenarios discussed earlier. There is a sharp contrast between the two modes of continuous operation for a pulse train of 12. Whereas ratio of pulsed to continuos operation is always smaller than unity for the first scenario, it is greater than unity for the second scenario. One can observe that the second scenario suggests a way of further reduction in radioactive inventory by reducing power of each pulse. Remember that the continuous operation in the second scenario effectively translates into lower pulse power vis-a-vis the pulsed mode for a given duty factor as long as duty factor is less than 100%. One can also infer that if it were possible to lower pulse power, one could achieve additional reduction in the radioactive inventory, on one hand, and, enhance the duty factor, on the other. In practical terms for ITER operation, this contrast suggests use of smaller power pulses, if physically possible, with a larger duty factor if one is looking to reduce radioactive inventory for a given fluence and total real time[7]. Obviously, the alternative scenario is contingent on the availability of power modulation in ITER.

III. EXPERIMENTAL TECHNIQUE

As discussed by Bartels[2] for stainless steel 316 activation, the largest contributions at shutdown come in the following order: ^{56}Mn ($t_{1/2}$=2.6h), followed by ^{52}V($t_{1/2}$=3.8 min), ^{58}Co ($t_{1/2}$=71d), ^{54}Mn($t_{1/2}$=10 months), ^{57}Co($t_{1/2}$=9 months), ^{28}Al ($t_{1/2}$=2.3 min), and ^{55}Fe ($t_{1/2}$=2.9 years). He suggests scenarios for reduction in radioactive inventory by taking credit for pulsed operation of ITER. The ITER EDA design is optimized around 1000s burn time[5]. We were interested in looking at the impact of pulsed operation for as many of these activities as possible. From the viewpoint of covering a large range of $t_{1/2}/p$ around the minima of Fig. 1, we looked around for potential products that fit this criteria along with permitting to take as small a pulse length as possible. To minimize activation of the neutron-source target and the neighboring structures, we decided not to exceed maximum irradiation time for a pulse train of ~ 30 min. Also, we decided on three duty factors of 10, 20 and 50%, at the most. The limiting number of pulses was set at ~10. This meant that for experimental data below $[t_{1/2}/p]_{minimum}$ ~ 2-5 (for d=0.1-0.5), we needed to include products with half life in the range of 12 minutes or lower too. As the unit pulse length was chosen as 3 min, it was important to include the half lives below 3 min too.

Sets of 6 foils each of niobium, iron, aluminum, vanadium, nickel, and magnesium were chosen for the measurements of the decay radioactivity of the following products: (i) ^{25}Na, and ^{24}Na of magnesium, (ii) ^{62m}Co, ^{62g}Co, ^{57}Ni, ^{58}Co, and ^{57}Co of nickel, (iii) ^{52}V, ^{51}Ti, and ^{48}Sc of vanadium, (iv)^{53m}Fe, and ^{56}Mn of iron, (v) ^{27}Mg, and ^{24}Na of aluminum, and (vi)^{90m}Y, and ^{92m}Nb of niobium. The half lives of these products vary from 1min (^{25}Na) to 271 d (^{57}Co). The pulse length was 3min. Table 1 summarizes half lives and prominent decay-γ energies of these products. Due to very short half life of products like ^{25}Na ($t_{1/2}$ = 1 min), ^{52}V (3.75 min), ^{62m}Co (1.5 min), ^{53m}Fe (2.58 min) etc., it was necessary to rapidly transfer the activated foils so as to be able to have enough counting on them before the activities decayed out. It was thus necessary to work with a pneumatic transport system (PTS). It was done, and we transported each foil set between an outer room and the irradiation target room pneumatically, as shown schematically in Fig. 2. A fresh set of foils was carefully placed in the same orientation inside the pneumatic tube each time before being zapped to the other end of the tube near the target where it was blocked by a stopper. A Nb foil inside each set directly faced the D-T target. The other five foils of iron, aluminum, vanadium, nickel, and iron followed in that order. This ensured that all the foils faced the same neutron spectra in different runs. A typical foil had a diameter of 10 mm and thickness of 1 mm.

As soon as an irradiation run was over, the sample foil set was retrieved through the PTS, and the activated foils were taken apart for counting on four γ-detectors of intrinsic germanium type. The first counting sweep, lasting ~5 min, included foils of nickel, vanadium, magnesium, and iron. The second counting sweep, lasting ~10 min, included foils of nickel, vanadium, aluminum, and iron. The third sweep, lasting ~20 min, covered nickel, vanadium, aluminum, and iron. The fourth sweep, lasting ~45 min or longer, included nickel, vanadium, niobium, and iron. Sometimes, there was a fifth run to improve counting statistics on some of the products and also to reduce the dead time counting losses.

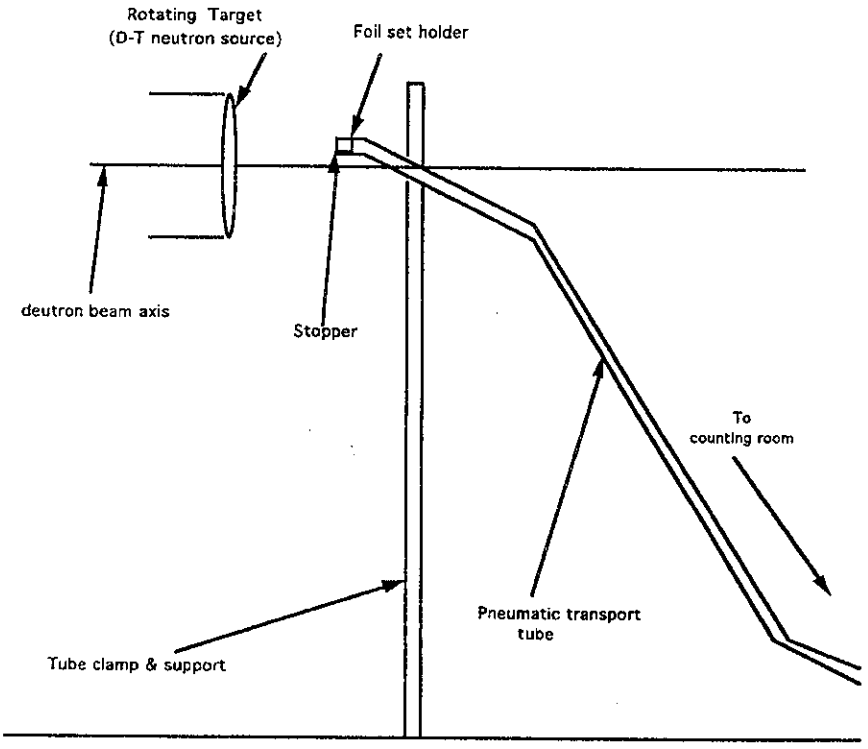

Schematic Representation of Pneumatic Transport System for Foil Despatch and Retrieval

Figure 2 Schematic view of layout of pneumatic transport tube system for dispatch and retrieval of the sample foil set for irradiation during an experimental run

Table 1 Selected foils, reactions, radioactive products, half lives, and decay γ-ray energies

Foil	Reaction	Product & γ-ray energy	Half-life $t_{1/2}$ & $t_{1/2}$/p@
Mg	$^{25}Mg(n,p)^{25}Na$	^{25}Na,975 keV	1min, 0.333
	$^{24}Mg(n,p)^{24}Na$	^{24}Na,1369 keV	15.02h, 300.4
Ni	$^{62}Ni(n,p)^{62m}Co$	^{62m}Co,1173keV	1.5min, 0.5
	$^{62}Ni(n,p)^{62g}Co$	^{62g}Co,1163 keV	13.9min, 4.63
	$^{58}Ni(n,2n)^{57}Ni$	^{57}Ni,1378 keV	36.0h, 720
	$^{58}Ni(n,p)^{58m+g}Co$	$^{58m+g}Co$,811keV	70.9d, 3.40 10^4
	$^{58}Ni(n,np/d)^{57}Co$	^{57}Co,122 keV	271d, 1.30 10^5
Fe	$^{54}Fe(n,2n)^{53m}Fe$	^{53m}Fe,701 keV	2.58min, 0.86
	$^{56}Fe(n,p)^{56}Mn$	^{56}Mn,847 keV	2.58h, 51.6
V	$^{51}V(n,\gamma)^{52}V$	^{52}V,1434 keV	3.75min, 1.25
	$^{51}V(n,p)^{51}Ti$	^{51}Ti,320 keV	5.8min, 1.93
	$^{51}V(n,\alpha)^{48}Sc$	^{48}Sc,984 keV	43.7h, 874
Al	$^{27}Al(n,p)^{27}Mg$	^{27}Mg,844 keV	9.46min, 3.15
	$^{27}Al(n,\alpha)^{24}Na$	^{24}Na,1369 keV	15.02h, 300.4
Nb	$^{93}Nb(n,\alpha)^{90m}Y$	^{90m}Y,202 keV	3.19h, 63.8
	$^{93}Nb(n,2n)^{92m}Nb$	^{92m}Nb,935 keV	10.15d, 4872

@ p is pulse length = 3 min

IV. EXPERIMENTAL TESTS

In all, there were 11 runs: 3 runs on day#1 (RUNs #1 through 3), 5 on day#2 (RUNs #4 through #8) , and 3 on day#3 (RUNs #9 through #11), as shown schematically in Figures 3 through 5. Each pulse, during runs with various pulse trains, had a length of 3 min. There were 5 runs, i.e., #3, #5, #6, #7, and #10, corresponding to '10-pulse' case, as shown schematically in Fig. 5. These runs were completed on different days. RUN#3, RUN#6, and #7 had almost constant source neutron intensity (or power) for all pulses. RUN#3 with a duty factor of 10% had a pulse of 3 min duration followed by 27 min of neutron-less interregnum. RUN#6, with a duty factor of 20%, allowed 12 min interval between two successive pulses. RUN#7 pertained to duty factor of 50% - a 3 min pulse was followed by a 3 min of cooling time (no-neutrons). RUN#5 was a single, continuous irradiation run lasting 30 min. This run was used as a reference continuous run for obtaining pulsed to continuous ratios of measured radioactive inventories. During RUN#10 (duty factor

= 20%), neutron source intensity ('power') was intentionally varied arbitrarily, from pulse to pulse, so as to make it quite random. There were four runs corresponding to 3 pulses, as shown schematically in Fig. 4. Out of four runs, i.e., RUN#2, #8, #9, and #11, only one run, i.e., RUN#2 (d=10%) had 'constant' power (source neutron intensity) for each pulse. For RUN#8 (d=20%), the power dropped from pulse#1 through #3 as follows: 1, 0.5, 0.2. For RUN#9 (d=20%), the power rose from pulse#1 through #3 as follows: 0.2, 0.5, 1.0. On the other hand, for RUN#11 (d=20%), the power went up from 0.5 to 1.0 and then dropped to 0.5. RUN#1 (d = 10%), had two pulses of the same amplitude that were separated by 27 min, as shown schematically in Fig. 3.

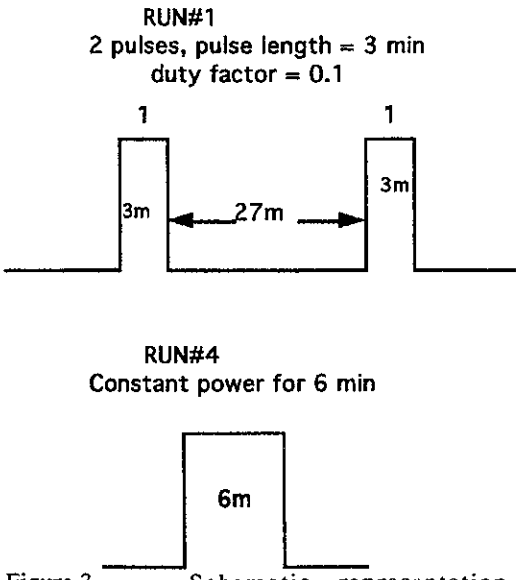

Figure 3 Schematic representation of experimental runs with a train of 2 pulses that include runs #1, and #4

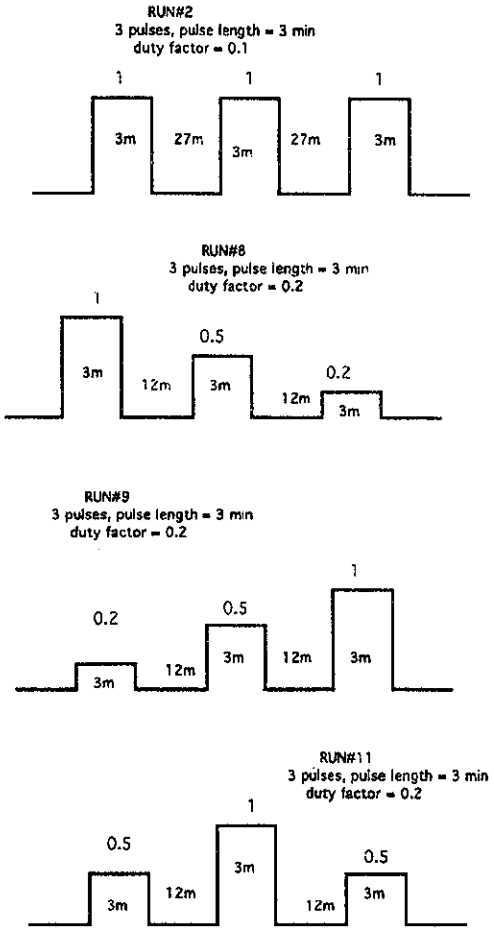

Figure 4 Schematic representation of experimental runs with a train of 3 pulses that include runs #2, #8, #9, and #11

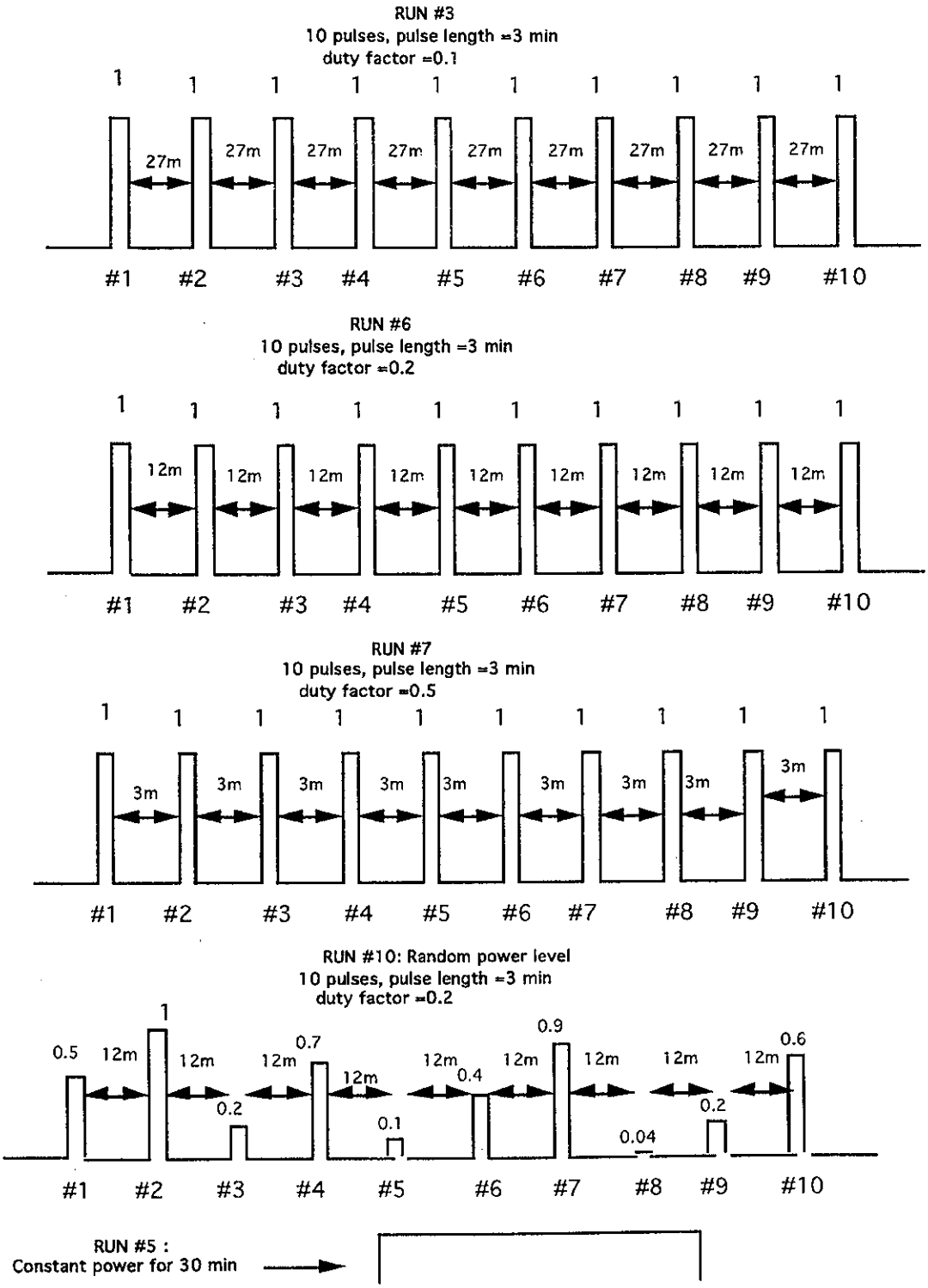

Figure 5 Schematic representation of experimental runs with a train of 10 pulses that include runs #3, #6, #10, #7, and #5

After each irradiation, γ-rays emitted from the samples were measured with Ge detectors linked to multi-channel pulse height analyzers. The data were recorded in a VAX-3100 Work Station at FNS. The γ pulse-height spectrum for a sample for each cooling time is processed by GENIE spectroscopy application system delivered by CANBERRA Inc. The measured γ-ray spectrum was then corrected for detector efficiency (ε) and attenuation (μ) of decay γ -rays emitted in a sample. The γ-ray emission rate for an individual γ-ray peak, E_{act}, as normalized by total MCS counts over a run, was then obtained[6,7]. As for error estimation on experimental measurements, it is to be recognized that a number of parameters affect counting statistics[6,7]. The primary parameters include: neutron flux, half life of γ-emitter, detector efficiency, cooling time, counting time, the relative orientation of the foil packet at the head of the PTS, activation cross-section and atom density. We attempted to achieve better than 5% accuracy on counts for majority of the γ-peaks. The total experimental error is, mostly, expected to be in the range of 2 to 10%.

V. EXPERIMENTAL ANALYSIS & DISCUSSION

The measured MCS spectra were used as a measure of time-dependent source neutron intensity. Figures 6 through 10 compare calculated and experimental ratios of inventories for pulsed to continuous operation as a function of half life of the product (expressed as $t_{1/2}/p$) for pulse trains of 2 (Fig. 6), 3 (Fig. 7), 10 members (Fig. 8 and 9), and 3 members with different power modulation (Fig. 10). Also shown are the plots with constant power pulses.

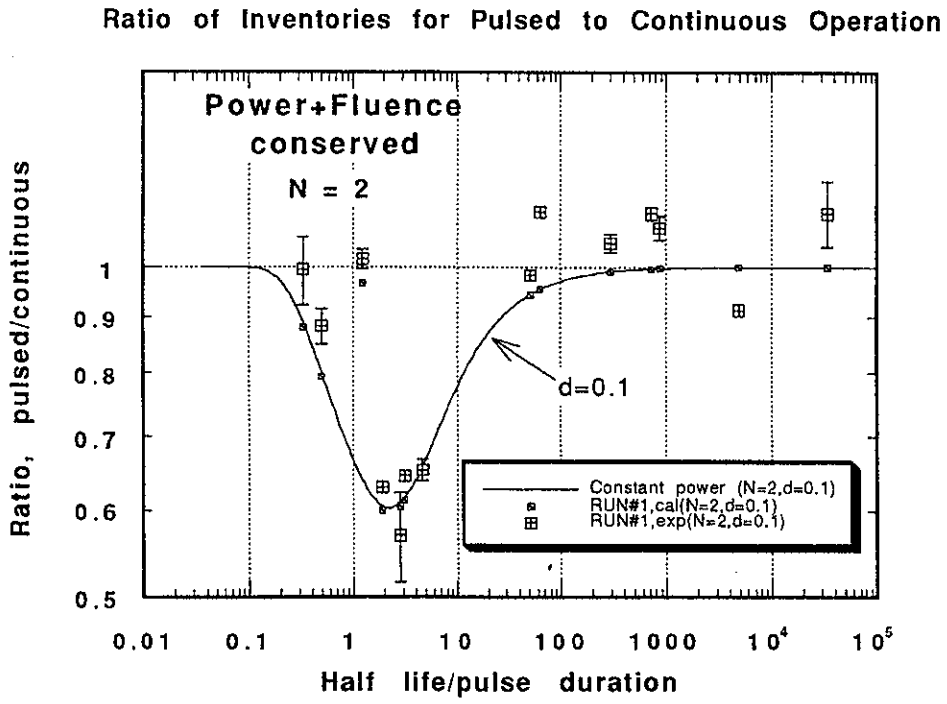

Fig. 6 Experimental and calculated ratios of inventories for pulsed to continuous operation for a pulse train comprising 2 pulses as a function of $t_{1/2}/p$ (half life/pulse duration)

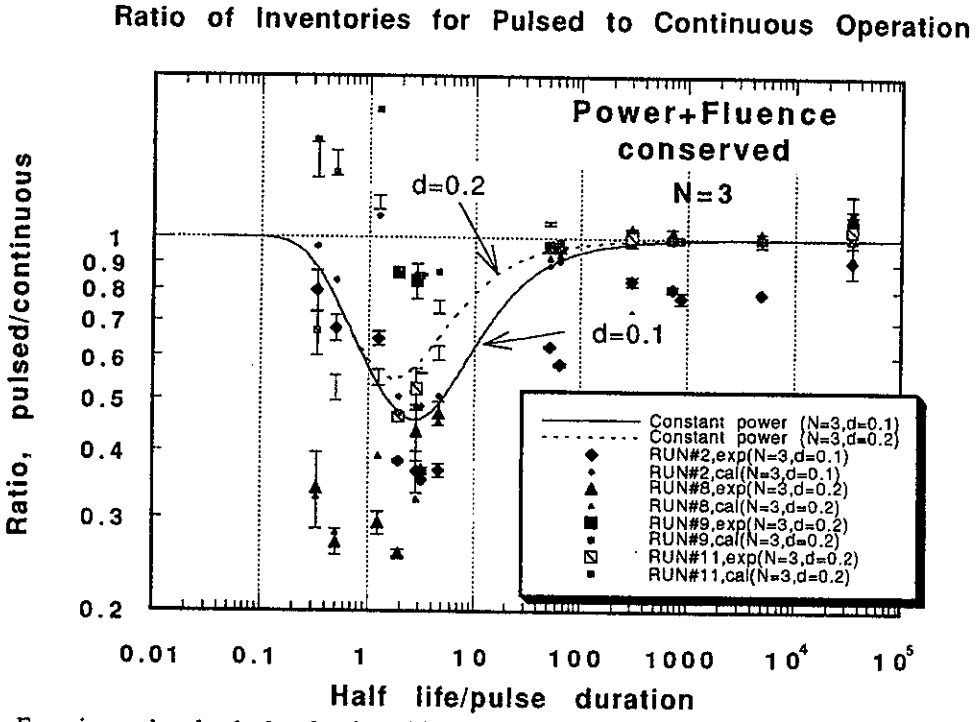

Fig. 7 Experimental and calculated ratios of inventories for pulsed to continuous operation for a pulse train comprising 3 pulses as a function of $t_{1/2}/p$

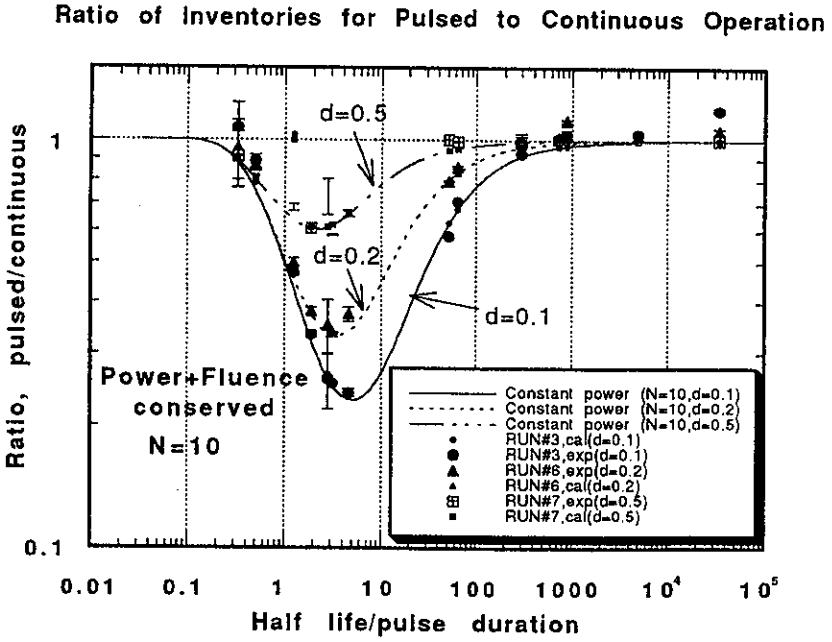

Fig. 8 Experimental and calculated ratios of inventories for pulsed to continuous operation for a pulse train comprising 10 pulses as a function of $t_{1/2}/p$

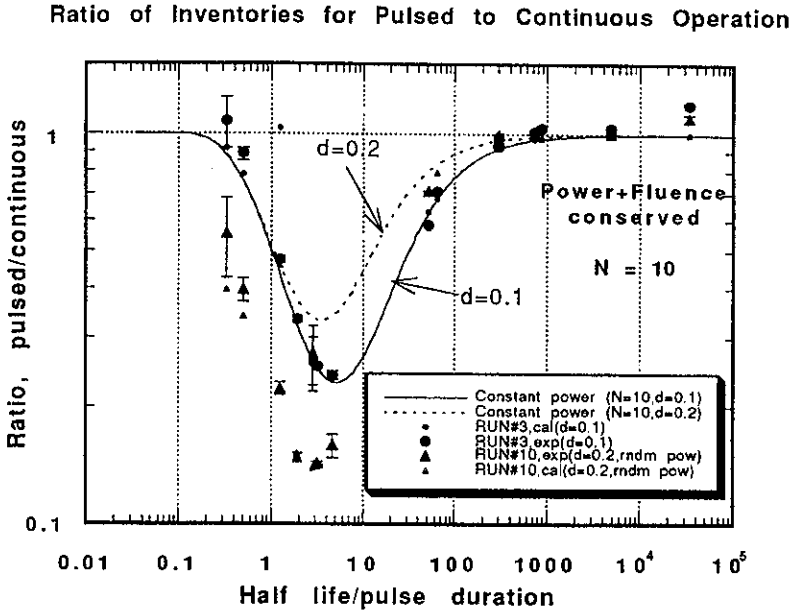

Fig. 9 Experimental and calculated ratios of inventories for pulsed to continuous operation for a pulse train comprising 10 pulses (including those with random power from pulse to pulse: RUN#10) as a function of $t_{1/2}/p$

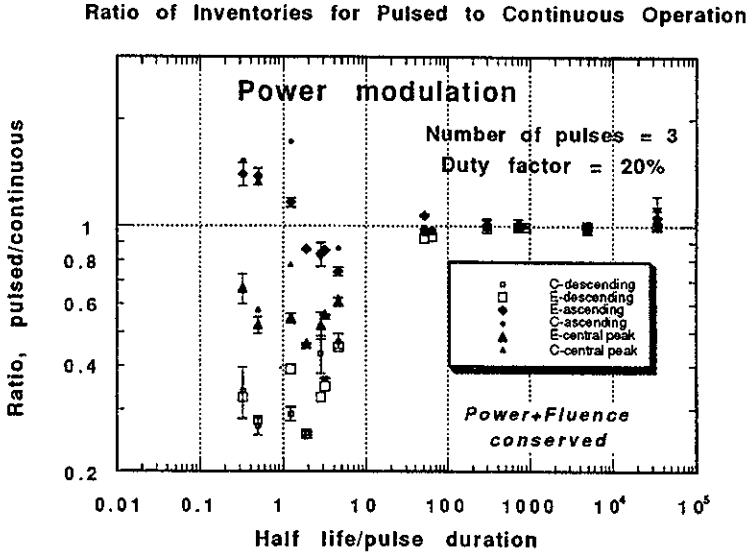

Fig. 10 Experimental and calculated ratios of inventories for pulsed to continuous operation for pulse trains comprising 3 pulses with power modulation: descending (RUN#8), ascending (RUN#9), and central peaking (RUN#11) as a function of $t_{1/2}/p$

The following remarks are in order:

- The 'constant power' cases, i.e., RUN#1 in Fig. 6, and RUN#3, #6, #7 in Fig. 8, show satisfactory agreement with constant power plots, and the calculated ratios are usually closer to these plots,
- The deviation from 'constant power' cases is particularly severe on products with smaller half lives

in that it results in large departures from the constant power plots. This is particularly true for RUNs#8, #9, and #11 in Fig. 3 (N=3), and RUN#10 in Fig. 9 (N=10)

• In fact, "random power" pulse trains show larger reduction in radioactive inventory: the ratio of inventories drops to ~0.14 for $t_{1/2}/p = 3.15$ (^{27}Mg) for a duty factor of 20% and a pulse train of 10, whereas it would have hit a minimum of ~0.33 for $t_{1/2}/p = 3.53$ for constant power level (see Fig. 9)

• Fig. 10 brings out clearly that it is important to know power carried by each pulse if power is not held constant. RUN#8 had 3 pulses with monotonically decreasing power ("descending" case). RUN#9 had 3 pulses with monotonically rising power ("ascending" case). RUN#11 had 3 pulses with the middle pulse having the largest power ("central peaking" case). Symblols C and E designate Calculated and experimental ratios respectively. As can be clearly seen from the Fig. 10, one can get a large uncertainty in predicting radioactive inventory, in t1/2/p range below ~5, under pulsed operation if one did not accurately know relative power levels of each pulse.

VI. CONCLUSION

Both the calculations and the experiments demonstrate that the pulsed operation leads to reduction in the radioactive inventories when both power and fluence are held constant. Also, the shapes of the pulses inside a pulse train impact the relative amount of radioactivity generated in the pulsed mode of operation. The reduction in the radioactive inventory with the pulsed mode operation grows with reduction in the duty factor. It follows that significant reduction in radioactive inventory can be accomplished by lowering duty factor, if power associated with each pulse is not changeable. But, as we described above while discussing two modes of continuous operation, if it were possible to lower pulse power, one could achieve additional reduction in the radioactive inventory, on one hand, and, enhance the duty factor, on the other.

As is widely known[7-14], it is observed that the pulsed mode operation reduces significantly the radioactivity levels at the end of operation as a function of duty factor and pulse duration as compared to the continuous operation case. The present experimental results confirm the reduction predicted by the analytical algorithms under pulsed mode irradiation.

In addition to the present experimental demonstration, we choose to highlight another important aspect of the pulsed mode scenario. In spite of our express efforts at controlling the source outputs as well as pulse shapes during various runs, we fell short on practically all occasions. This brings us to ask the following question : *how accurately could we control the power level and how could we realize the ideal pulsed mode operation sequences as "scheduled" for ITER?* One needs to answer this question satisfactorily along with a design safety margin. The designers and safety specialists need to fold these considerations into the design of ITER for reflecting a greater degree of realism, while predicting estimates of radioactive inventories during planned operational schedules of ITER.

REFERENCES

1. M. Zucchetti, "Impurity Concentration Limits and Activation in Fusion Reactor Structural Materials," *Fusion Technology*, **19**, 294 (1991).

2. H.W. Bartels, "Taking Credit for pulsed operation in ITER in the activation calculations", *Interoffice memorandum*, ITER JCT San Diego Office (March 24, 1994)

3. H. Attaya, "Radioactivity Computation of Steady State and Pulsed Fusion Reactor Operation,"*Fusion Engineering and Design*, **28**, 571 (1995).

4. Q. Wang, and D.L. Henderson, "Pulsed Activation Analyses of the ITER Blanket Design Options Considered in the Blanket Trade-off Study," *Fusion Engineering and Design*, **28**, 579 (1995).

5. G. Saji, Private Communication (June 21, 1994).

6. A. Kumar et al., "Decay Radioactivity Induced in Plasma-facing materials by Deuterium-Tritium neutrons ," *Fusion Technology*, **28**, 99 (1995).

7. A. Kumar, Y. Ikeda, M.Z. Youssef, M.A. Abdou, Y. Uno, and H. Maekawa, "Development and Demonstration of Techniques for Measurement of Neutron Induced Radioactivity," *ITER/US/95/IV-BL-13 report on subtask#2 of ITER Task T16* (December 1994).

8. H. Attaya, Y. Gohar, and D. Smith, "US-ITER Activation Analysis", *Fusion Technology*, **19**, 1837 (1991).

9. S.E. Spangler, J.E. Sisolak, and D.L. Henderson, "Calculational Models for the Treatment of Pulsed/Intermittent Activation within Fusion Energy Devices", *Fusion Engineering and Design*, **28**, 349 (1993).

10. J.E. Sisolak, S.E. Spangler, and D.L. Henderson, "Pulsed/Intermittent Activation in Fusion Energy Reactor System", *Fusion Technology*, **21**, 2145 (1992).

11. L.P. Ku, "Radioactivation Characteristics for the Tokamak Fusion Test Reactor", *Fusion Technology*, **4**, 586 (1983).

12. A. Kumar, C. Sahraoui, and S. Azam, "Results from Recent Experiments at the LOTUS Facility," *Fusion Technology*, **15**, 1315 (1989).

13. Y. Ikeda et al., "Measurements of Induced Activity in Type 316 Stainless Steel by Irradiation in D-T Neutron Fields," *JAERI-M 83-177* report (1983)..

14. Y. Ikeda et al., "Measurements of Induced Activity in Type 316 Stainless Steel by Irradiation in D-T Neutron Fields," *Fusion Technology*, **8**, 1466 (1985).